



Supplement of

The impact of unimolecular reactions on acyl peroxy radical initiated isoprene oxidation

Ida Karppinen et al.

Correspondence to: Nanna Myllys (nanna.myllys@helsinki.fi)

The copyright of individual parts of the supplement might differ from the article licence.

Other calculated unimolecular reaction rate coefficients

Table S1 presents the rest of the calculated unimolecular reaction rates for the acyl peroxy radicals studied. These reactions are also illustrated in Figure S1. For *acr*-APR, *cyc3*-APR and *cyc4*-APR 1,4 H-shifts, the reaction product decomposed similarly to *ace*-APR 1,4 H-shift. This decomposition led to the formation of a hydroperoxy radical and a ketene corresponding to the reacting APR structure.

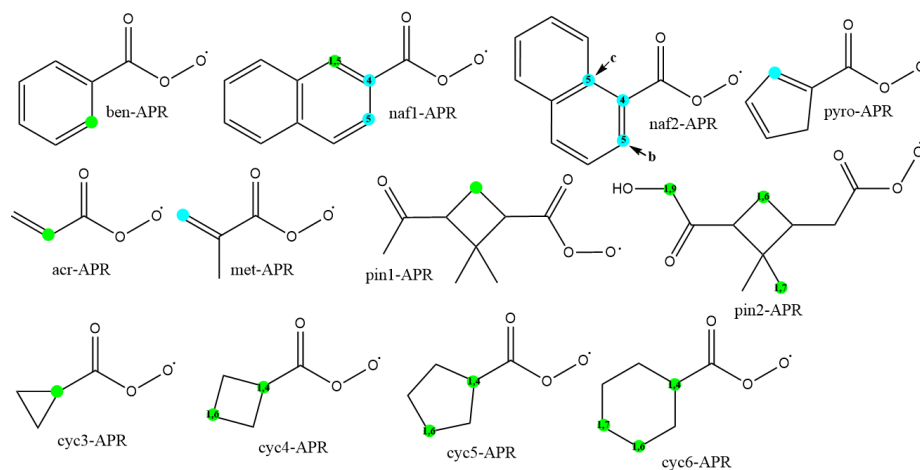


Figure S1: APR structures and studied unimolecular reactions corresponding to the results in Table S1. Reactions are marked with dots, green for H-shifts and blue for endoperoxide ring formations. For clarification, the prefixes for structures with multiple calculated rates are also marked.

Table S1: Calculated energy barrier heights (ΔE^{TS} in kcal/mol), Eckart tunneling coefficients (κ_t) for H-shifts and unimolecular MC-TST reaction rate coefficients (k_{uni} in s^{-1}) at 298 K of other unimolecular reactions for the studied APRs.

| Radical | Reaction | ΔE^{TS} | κ_t | k_{uni} |
|----------|-----------------------------|------------------------|------------|------------------------|
| Acr-APR | 1,4 H-shift ^a | 42.34 | 2 | 1.75×10^{-18} |
| Met-APR | 5-endoperoxide | 21.58 | - | 2.71×10^{-4} |
| Ben-APR | 1,5 H-shift | 29.76 | 9 | 2.58×10^{-9} |
| Pyro-APR | 5-endoperoxide | 23.18 | - | 9.30×10^{-6} |
| Cyc6-APR | 1,4 H-shift | 22.86 | 42 | 4.79×10^{-3} |
| | 1,6 H-shift | 24.51 | 32 | 6.19×10^{-5} |
| | 1,7 H-shift | 27.12 | 32 | 4.36×10^{-7} |
| Cyc5-APR | 1,4 H-shift | 22.87 | 40 | 1.73×10^{-3} |
| | 1,6 H-shift | 22.22 | 91 | 1.81×10^{-3} |
| Cyc4-APR | 1,4 H-shift ^a | 38.23 | 3 | 9.63×10^{-15} |
| | 1,6 H-shift | 27.48 | 238 | 1.24×10^{-6} |
| Cyc3-APR | 1,4 H-shift ^a | 39.72 | 2 | 1.81×10^{-16} |
| Pin1-APR | 1,5 H-shift | 24.42 | 26 | 5.52×10^{-5} |
| Pin2-APR | 1,6 H-shift | 22.88 | 66 | 9.26×10^{-4} |
| | 1,7 H-shift | 22.79 | 163 | 1.35×10^{-3} |
| | 1,9 H-shift | 24.96 | 101 | 6.03×10^{-6} |
| Naf1-APR | 1,5 H-shift | 29.57 | 7 | 1.67×10^{-9} |
| | 4-endoperoxide | 23.59 | - | 6.81×10^{-6} |
| | 5-endoperoxide | 22.55 | - | 1.73×10^{-5} |
| Naf2-APR | 4-endoperoxide | 19.64 | - | 5.59×10^{-3} |
| | 5-endoperoxide ^b | 19.94 | - | 1.53×10^{-3} |
| | 5-endoperoxide ^c | 28.89 | - | 3.03×10^{-10} |

^a Reaction product decomposes. ^{b&c} See Figure S1.

Comparison of ω B97X-D and M06-2X functionals for calculating rates for reactions between isoprene and APRs

Table S2 presents the calculated bimolecular reaction rate coefficients for the reactions of isoprene with ace-, pro- and ben-APR with two different functionals, ω B97X-D and M06-2X, using MC-TST. Also, the LC-TST rates calculated using the ω B97X-D functional are included.

Table S2: Calculated energy barrier heights (ΔE^{TS} in kcal/mol) and bimolecular reaction rate coefficients (k_{bi} in cm^3s^{-1}) at 298 K for ace-APR R4, pro-APR and ben-APR R1 reactions with isoprene calculated at the DLPNO-CCSD(T)/aug-cc-pVTZ// ω B97X-D/6-31+G* (LC-TST and MC-TST) and DLPNO-CCSD(T)/aug-cc-pVTZ//M06-2X/6-31+G* level (MC-TST).

| Radical | Reaction | Functional | Theory | ΔE^{TS} | k_{bi} |
|---------|----------|-----------------|--------|------------------------|-----------------------|
| Ace-APR | R4 | ω B97X-D | MC-TST | 2.8 | 1.1×10^{-17} |
| | | ω B97X-D | LC-TST | | 1.3×10^{-17} |
| | | M06-2X | MC-TST | 2.8 | 6.0×10^{-18} |
| Pro-APR | R1 | ω B97X-D | MC-TST | 1.3 | 1.3×10^{-16} |
| | | ω B97X-D | LC-TST | | 8.5×10^{-17} |
| | | M06-2X | MC-TST | 1.4 | 2.8×10^{-17} |
| Ben-APR | R1 | ω B97X-D | MC-TST | 0.1 | 1.6×10^{-15} |
| | | ω B97X-D | LC-TST | | 9.1×10^{-16} |
| | | M06-2X | MC-TST | 0.3 | 4.9×10^{-16} |

PES graphs for reactions R1 and R4 between isoprene and OH

The PES graphs for the reactions R1 and R4 between isoprene and OH calculated with two different functionals, ω B97X-D and M06-2X, are presented in Figures S2 and S3.

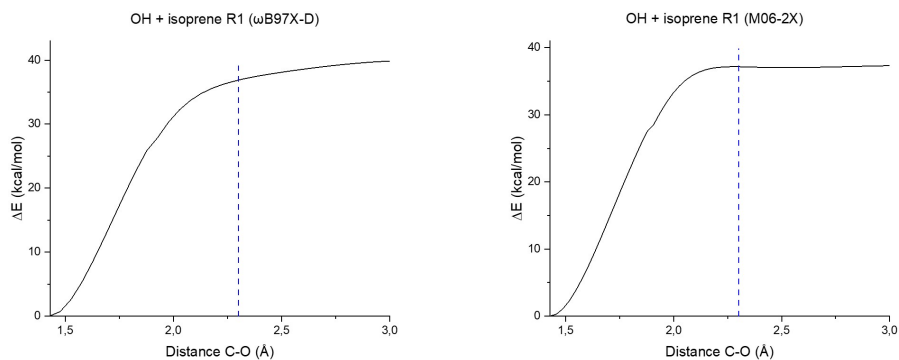


Figure S2: PES graphs for reaction R1 between isoprene and OH calculated with ω B97X-D and M06-2X functionals. Energies are relative to the equilibrium structure. Blue dashed line shows C–O bond distance for TS structure optimized at the M06-2X/6-31+G* level.

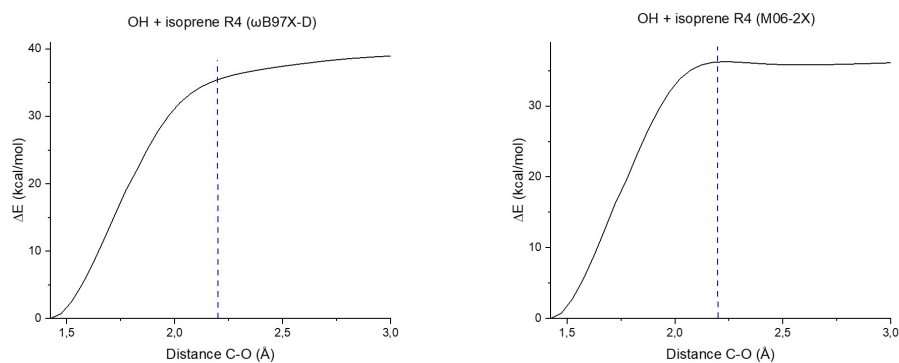


Figure S3: PES graphs for reaction R4 between isoprene and OH calculated with ω B97X-D and M06-2X functionals. Energies are relative to the equilibrium structure. Blue dashed line shows C–O bond distance for TS structure optimized at the M06-2X/6-31+G* level.

Energy diagrams for ace-APR and OH reactions R1 with isoprene

Energy diagrams are presented in Figure S4. Energies for reactants, complex, TS and product were calculated at the DLPNO-CCSD(T)/aug-cc-pVTZ// ω B97X-D/6-31+G* level for ace-APR and DLPNO-CCSD(T)/aug-cc-pVTZ//M06-2X/6-31+G* level for OH.

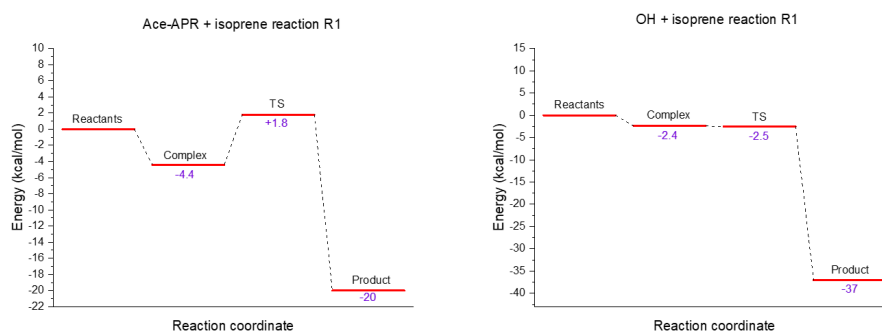


Figure S4: Energy diagrams for ace-APR and OH reactions R1 with isoprene calculated at the DLPNO-CCSD(T)/aug-cc-pVTZ// ω B97X-D/6-31+G* and DLPNO-CCSD(T)/aug-cc-pVTZ//M06-2X/6-31+G* level, respectively.